

---

1 **Comparison of water-soluble and insoluble organic compositions attributing to different light**  
2 **absorption efficiency between residential coal and biomass burning emissions**

3 Lu Zhang <sup>1,2</sup>, Jin Li <sup>1</sup>, Yaojie Li<sup>1</sup>, Xinlei Liu <sup>1</sup>, Zhihan Luo <sup>1</sup>, Guofeng Shen <sup>1, \*</sup>, and Shu Tao <sup>1,3</sup>

4 1. *Laboratory for Earth Surface Process, College of Urban and Environmental Sciences, Peking*  
5 *University, Beijing 100871, China*

6 2. *Hong Kong Polytechnic University, Department of Civil & Environmental Engineering,*  
7 *Kowloon, Hong Kong, China*

8 3. *College of Environmental Science and Technology, Southern University of Science and*  
9 *Technology, Shenzhen 518055, China*

10

11 \* *Corresponding author: Dr. Guofeng Shen, Peking University, Email: gfshe12@pku.edu.cn*

---

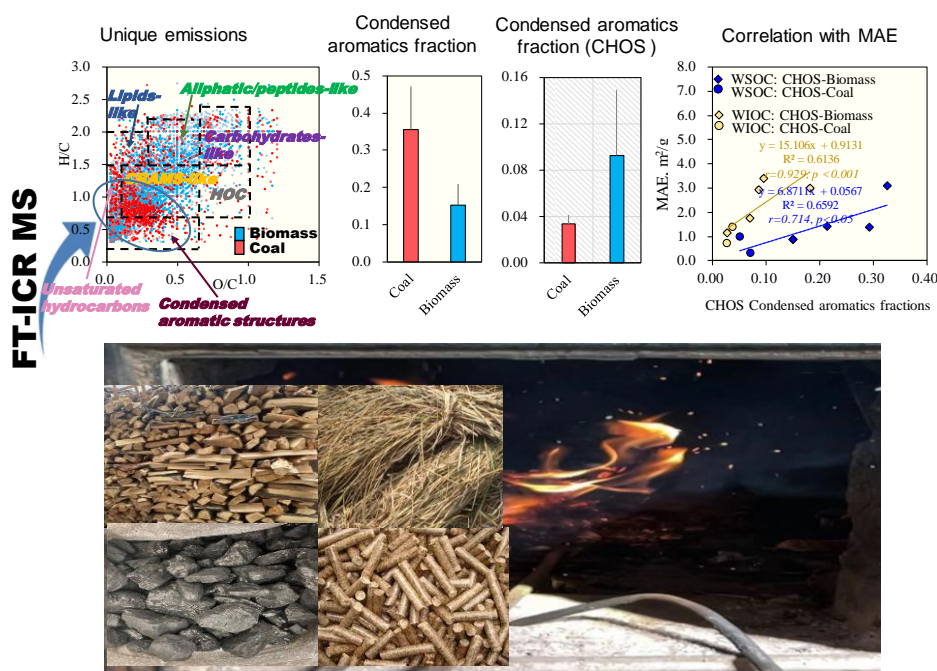
## 12 Abstract

13 There are growing concerns about the climate impacts of absorbing organic carbon (also known as  
14 Brown Carbon, BrC) in the environment, ~~however, they~~ yet its chemical composition and association  
15 with the light absorption ~~ability of BrC capabilities~~ remain poorly understood. ~~In this study, This~~  
16 study characterized focusing on one major source of BrC, water-soluble and water-insoluble organic  
17 carbon (WSOC, WISOC) from residential solid fuel combustion ~~were characterized~~ at the molecular  
18 level; and evaluated ~~for~~ their quantitative relationship with mass absorption efficiency (MAE). The  
19 MAE values at  $\lambda=365$  nm from biomass burning were significantly higher than those from coal  
20 ~~combustion~~ combustion ( $p<0.05$ )s. Thousands of peaks were identified in the m/z range of 150-800,  
21 with the most intense ion peaks occurring between ~~of~~ 200-500 m/z for WSOC and 600-800 m/z for  
22 WISOC, respectively. The CHO group predominated ~~was the most abundant component~~ in the  
23 WSOC extracts from biomass burning emissions ~~compared to coals;~~ while sulfur-containing  
24 compounds (SOCs) including CHOS and CHONS ~~while sulfur-containing compounds~~  
25 ~~(CHOS+CHONS, SOCs)~~ were more intense in the WISOC extracts, particularly from ~~specially in~~  
26 coal emissions. Emissions of the CHON group were positively correlated with the fuel nitrogen  
27 content ( $r=0.936$ ,  $p<0.05$ ), explaining their higher abundance ~~which explained higher CHON~~  
28 ~~emissions in~~ coal emissions compared ~~to~~ biomass ~~burning emissions~~. The SOCs emissions were  
29 ~~were~~ more predominant in during flaming phases, ~~as seen from~~ as indicated by a positive correlation  
30 ~~between SOCs and~~ with modified combustion efficiency (MCE) ( $r=0.750$ ,  $p<0.05$ ). The unique  
31 formulas of coal combustion aerosols were in the lower H/C and O/C regions with higher  
32 unsaturated compounds in the van Krevelen (VK) diagram. In ~~WISOC~~ WIOC extracts, coal  
33 combustion emissions ~~had contained~~ significantly higher fractions of condensed aromatics (32-  
34 59%), compared to ~~which was~~ only 4.3-9.7% in biomass burning emissions. However, The ~~the~~

35 CHOS group in biomass burning emissions was characterized by larger condensed aromatic  
 36 compound fractions ~~compared to than those in~~ coal combustion. The CHOS aromatic compound  
 37 fractions were positively correlated with MAE values, in both WSOC ( $r=0.714$ ,  $p<0.05$ ) and  
 38 ~~WISOC~~WIOC extracts ( $r=0.929$ ,  $p<0.001$ ), suggesting ~~the abundance of CHOS aromatic~~these  
 39 compounds significantly ~~explained~~contributed to MAE variabilities across ~~the diffedifferentrent~~  
 40 fuels.

41 *Keywords:* light absorption properties, atmospheric aerosols, N-containing compounds, S-  
 42 containing compounds, water-soluble compounds, water-insoluble compounds.

43 **TOC**



44 **1. Introduction**

45 Light-absorbing organic carbon (OC), known as Brown Carbon (BrC), attracts growing  
 46 concerns due to its direct radiative impact on climate change (Laskin et al., 2015; Wang et al., 2022).  
 47 The global simulations suggested that BrC may contribute nearly 20% of the surface organic aerosol  
 48 (OA) burden (Jo et al., 2016), and accounted for 19% of the light absorption by anthropogenic

---

49 aerosols (Feng et al., 2013). BrC ~~can be~~originates from ~~various diverse~~ sources, including primary  
50 emissions ~~sources such as~~from coal combustion, biomass burning, and vehicular emissions (Du et  
51 al., 2014; Olson et al., 2015; Bond, 2001; Sun et al., 2017; Chen and Bond, 2010), ~~and~~ ~~s~~Secondary  
52 processes ~~such as like~~ the oxidation of volatile organic compounds ~~would also generate considerable~~  
53 ~~BrC~~ (Guan et al., 2020; Laskin et al., 2015). Among these sources, residential solid fuel burning  
54 ~~produce~~produced large amounts of BrC, accounting for 74% of the total anthropogenic primary  
55 emissions (Xiong et al., 2022).

56 Some efforts have been made to explore the BrC physiochemical properties in residential  
57 emissions. For example, water-soluble organic carbon (WSOC) and methanol-soluble organic  
58 carbon (MSOC) were analyzed in primary emissions from combustions of crop straw, wood fuel,  
59 and some coals (Park and Yu, 2016). Available studies suggested that the optical properties of  
60 primary BrC varied ~~largely significantly, being~~ influenced by ~~many numerous~~ factors ~~including, such~~  
61 ~~as~~ inherent fuel properties and combustion conditions. Mass absorption efficiency (MAE) is a key  
62 parameter in assessing ~~the~~ direct radiative forcing of ~~the~~ light-absorbing carbonaceous aerosols  
63 (Huo et al., 2018). ~~It was found that water-soluble BrC derived from bituminous coals had higher~~  
64 ~~MAE values than anthracites (Tang et al., 2020). However, the specific chemical components~~  
65 ~~responsible for the differences in light absorption among various fuel types are not yet fully~~  
66 ~~understood, especially at the molecular level. The water-soluble BrC from bituminous coals were~~  
67 ~~found to have higher MAE values than anthracites (Tang et al., 2020); however, less well understood~~  
68 ~~are the chemical components, at the molecular level, responsible for light absorption differences~~  
69 ~~among different fuels.~~ It was also reported that the mass absorption of water-insoluble organic  
70 carbon (~~WISOC~~WIOC) could be even greater than that of the water-soluble ones (Chen and Bond,  
71 2010; Huang et al., 2018). ~~However, there is limited, but little~~ information ~~is~~ available ~~on~~ ~~regarding~~  
72 ~~their~~ chemical components ~~of them.~~ ~~Considering~~ ~~Given the significant variation in that~~ BrC light

73 absorption ~~varied dramatically among the~~across different fractions ~~and emitted from different~~  
74 ~~various~~ fuels (Xie et al., 2017), detailed information of a comprehensive characterization, including  
75 the chemical and optical characteristics of the BrC fractions (~~including~~both water-soluble and  
76 water-insoluble ~~ones~~) from the combustion source, is needed.

77 ~~In this study,~~This study investigated the chemical compositions and light absorption abilities  
78 of WSOC and WISOCWIOC in smoke particles ~~produced~~generated from the burning of coals with  
79 different maturity, raw biomass fuels, and biomass pellets in traditional and improved stoves,  
80 ~~were investigated for their chemical compositions and light absorption abilities.~~The use of biomass  
81 pellets has been heavily promoted over the last several years to mitigate air pollutant emissions from  
82 traditional solid fuels, and emission characteristics from improved stoves could be different from  
83 traditional ones. Optical property variations were quantitatively assessed and analyzed ~~for to explore~~  
84 their association with chemical components. Furthermore, uUnique molecules and fingerprints for  
85 coal and biomass sources were discussed, ~~that which~~ is critical in pollution source appointment.

## 86 2. Materials and methods

### 87 2.1 Laboratory ~~Combustion~~combustion ~~Emission~~ Experiment~~experiment~~

88 In ~~this the present~~ study, a total of fourteen types of coals with ~~different~~varying maturity  
89 degrees, five types of biomass ~~pellet~~pellets, and twelve types of raw biomass were examined using  
90 a laboratory combustion system. Two types of stoves, including a traditional stove (TS) and an  
91 improved stove (IS), were utilized for the experiments.~~tested in two stoves (one traditional stove~~  
92 ~~(TS) and an improve stove (IS)) in the laboratory combustion system.~~ The thirty-four fuel-stove  
93 combinations are listed in ~~the~~Table S1. The combustion tests were ~~conducted~~performed in a  
94 specially designed system ~~equipped~~with real-time online monitors (Thermo Scientific Inc., Bremen,  
95 Germany), which are capable of continuously measuring gaseous pollutants, including CO, CO<sub>2</sub>,

96 hydrocarbons (HC), and nitrogen oxide (NO<sub>x</sub> including NO and NO<sub>2</sub>) ~~online monitor (Thermo~~  
97 ~~Scientific Inc., Bremen, Germany)~~. PM<sub>2.5</sub> (particles with aerodynamic diameters ≤2.5 μm) was  
98 collected at a flow rate of 16.7 L/min with the quartz filters. Fuel properties including moisture  
99 (M<sub>ad</sub>, %), volatile matter content (V<sub>daf</sub>, %), ash content (A<sub>ad</sub>, %), lower heating value (LHV, MJ/kg),  
100 and contents of carbon (C, %), hydrogen (H, %), nitrogen (N, %), and sulfur (S, %) are tested, and  
101 listed in Table S1. Details of stove construction and combustion processes were available in Zhang  
102 et al., (2022).

103 Modified combustion efficiency (MCE) was calculated by integrating the incremental  
104 concentrations of CO<sub>2</sub> and CO as:

$$105 \quad \text{MCE} = \frac{\text{CO}_2}{\text{CO}_2 + \text{CO}}$$

106 where CO<sub>2</sub> and CO represent the excess molar mixing ratios of CO<sub>2</sub> and CO, respectively  
107 (Pokhrel et al., 2016). The MCE values indicate different phases of combustion: approximately 1  
108 during flaming, and between 0.7-0.9 during smoldering (Yokelson et al., 1997)

## 109 2.2 Bulk carbon and UV-vis absorption spectra

110 For each sample, a 4.9 cm<sup>2</sup> filter was extracted ultrasonically with 10 mL Milli-Q water (18.2  
111 MΩ) for 30 min, and then the supernatant was separated. The extraction process was repeated twice,  
112 and the extracts were combined ~~to obtain WSOC~~. The water extract was then filtered via a 0.22 μm  
113 polytetrafluoroethylene (PTFE) filter to obtain WSOC. Due to the inefficiency of water in extracting  
114 BrC, the insoluble PM components remaining on the sample filter were freeze-dried and subjected  
115 to methanol extraction through sonication. The resulting extract was then filtered using a PTFE filter,  
116 yielding a water-insoluble fraction referred to as WIOC in the following text. ~~The insoluble PM~~  
117 ~~components that remained on the sample filter were further freeze-dried and extracted with~~

118 ~~methanol via sonication and then filtered via a PTFE filter to obtain water insoluble fraction.~~ The  
 119 carbon content of WSOC was analyzed with a total organic carbon (TOC) analyzer (TOC-Lcph/cpn,  
 120 SHIMADZU, Japan), and the ~~WISOC~~ was ~~calculated~~ determined by as OC subtracting WSOC from  
 121 the total OC loaded on the same 4.9 cm<sup>2</sup> area, given that the methanol extraction efficiency for all  
 122 combustion samples ~~were was~~ up to 90% ~~as proved previously~~ (Zhang et al., 2022). The element  
 123 carbon (EC) and OC ~~was were~~ measured using a thermal-optical analyzer (Sunset OC/EC analyzer)  
 124 with an interagency monitoring of protected visual environments (IMPROVE) program.

125 The light absorption spectra of the water and methanol extracts were measured between 200  
 126 nm and 600 nm by UV-vis spectrophotometer (UV-2600, Shimadzu, Japan) at a step size of 1 nm.  
 127 MAE values of WSOC and WISOC/WIOC at the wavelength of  $\lambda$  ( $MAE_{\lambda, \text{wsoc}}$ ;  $MAE_{\lambda, \text{wisoewioc}}$ )  
 128 were calculated as following equation (Li et al., 2019):

$$129 \quad MAE_{\lambda, \text{wsoc}} = A_{\lambda, \text{wsoc}} \times \ln(10) / (C_{\text{wsoc}} \times L); \quad MAE_{\lambda, \text{wisoewioc}} = A_{\lambda, \text{wisoewioc}} \times \ln(10) / (C_{\text{wisoewioc}} \times L)$$

131 where  $A_{\lambda, \text{wsoc}}$  and  $A_{\lambda, \text{wisoewioc}}$  is the light absorption value of WSOC extract and  
 132 WISOC/WIOC extract at a wavelength of  $\lambda$ , respectively; C is the concentration of WSOC (or  
 133 WISOC/WIOC), and L is the optical path length, which is 0.01 m in this study. It is important to  
 134 note that the reported light absorption of WISOC/WIOC in this study was underestimated, while  
 135 such underestimation is insignificant due to the high extraction efficiency. In this study, the MAE  
 136 values of extractable OC at  $\lambda$  of 365 nm ( $MAE_{365, \text{wsoc}}$  ~~& and~~  $MAE_{365, \text{wisoewioc}}$ ) were discussed.

137 Absorption Ångström exponent (AAE) values were determined based on the following  
 138 equation (Li et al., 2019; Li et al., 2020):

$$139 \quad A_{\lambda} = K_{\lambda}^{-AAE}$$

140 where K is a constant and AAE is obtained through the linear regression of  $\lg(A_{\lambda})$  against  $\lg \lambda$   
 141 (Fig S1). Wavelength A wavelength of 300-400 nm is chosen according to the published literature

---

142 (Yue et al., 2022), and the goodness of fit for all the samples in this study is greater than an  $r^2$  of  
143 0.99.

### 144 2.3 Molecular composition analysis FT-ICR MS Analysis

145 For further molecular composition analysis, the WSOC and WIOC extracts from seven selected  
146 source samples were subjected to Fourier-transform ion cyclotron resonance mass spectrometry (FT-  
147 ICR MS) coupled with electrospray ionization (ESI).~~The WSOC and WIOC extract from seven~~  
148 ~~selected source samples were selected for further FT-ICR MS analysis.~~ These samples included two  
149 types of coals (high volatile bituminous coal, HVB; medium volatile bituminous coal, MVB)  
150 combusted in TS, two types of raw biomass (rice straw and pine wood) combusted in TS, pine wood  
151 combusted in IS, and two types of biomass pellets (crop straw pellet and pine wood pellet)  
152 combusted in IS as noted in SI. FT-ICR MS has been successfully applied for the molecular-level  
153 characterization of compounds (Bianco et al., 2018) due to its ultrahigh resolution and mass  
154 accuracy. ESI is well-adopted to characterize soluble aerosols, especially for the detection of polar,  
155 hydrophilic molecules like humic-like substances (HULIS)-type compounds (Wozniak et al., 2008),  
156 because it is a “soft” ionization technique generating minimal analyte fragments, and thus can detect  
157 intact molecules of compounds. Therefore, the negative ESI-FT-ICR was applied here to determine  
158 the molecular compositions of WSOC and ~~WISOC~~WIOC from combustion samples from different  
159 solid fuels. The methanol extracts were evaporated to dryness under a gentle stream of nitrogen and  
160 then dissolved with Milli-Q water. The WSOC and water-reconstituted ~~WISOC~~WIOC were  
161 submitted to solid-phase extraction (SPE) using Bond Elut PPL (500 mg, 6 mL, Agilent, U.S.A.).  
162 Before the extraction, the PPL cartridges were sequentially conditioned with 12 mL methanol and  
163 12 mL Milli-Q water containing 0.05% hydrochloric acid (HCl). The extract was adjusted to pH=2  
164 using HCl to remove inorganic ions and was then loaded onto the PPL cartridges at a rate of 5



---

165 mL/min. Cartridges were washed with 18 mL Milli-Q water containing 0.05% HCL to remove salt  
166 and then dried under pure nitrogen. Analytes were eluted with 12 mL methanol, and the combined  
167 eluates were concentrated to 1 mL. Then the molecular characterization was conducted using a 15T  
168 SolariX XR FT-ICR MS (Bruker Daltonik GmbH, Bremen, Germany) in the negative ESI mode.  
169 The capillary inlet voltage was set at -4.0 kV and ion accumulation time was set to 0.06 S. There  
170 were 300 continuous 4 M data FT-ICR transients added to improve the signal-to-noise ratio. The  
171 FT-ICR MS was calibrated with 10 mmol/L sodium formate in advance, and internal standard  
172 calibration with soluble organic matter (known molecular formula) was performed after the test.  
173 Finally, <1 ppm absolute mass error was achieved. Data processing details are described in the  
174 Supporting Information (SI).

### 175 3. Result and discussion

#### 176 3.1 Optical characteristics of WSOC and ~~WISOC~~WIOC

177 MAE is an important parameter reflecting the light absorption capability of the carbonaceous  
178 aerosols. The MAE<sub>365, WSOC</sub> of aerosols from residential ~~source~~sources in this study ranged from  
179 0.21 to 3.1 m<sup>2</sup>/g with an average of 1.3±0.7 m<sup>2</sup>/g. MAE values of extractable OC in this study were  
180 lower than that of 11.3 m<sup>2</sup>/g for pure BC aerosols (Bond and Bergstrom, 2006) and also lower than  
181 that from the filter-based MAE values of OC of 0.16-13 m<sup>2</sup>/g from residential sources (Zhang et al.,  
182 2021b). A significant difference ( $p<0.05$ ) of MAE<sub>365, WSOC</sub> was observed among the different fuels  
183 (Fig.1). The MAE<sub>365, WSOC</sub> of raw biomass combustion derived aerosols averaged at 1.7±0.8 m<sup>2</sup>/g,  
184 which was significantly higher ( $p<0.05$ ) than those from coal smoke (0.93±0.44 m<sup>2</sup>/g) and biomass  
185 pellet smoke (1.2±0.6 m<sup>2</sup>/g). The MAE<sub>365, ~~WISOC~~WIOC</sub> ~~was ranged from 0.49 to 6.6 m<sup>2</sup>/g with an in~~  
186 ~~the range of 6.6±0.5 m<sup>2</sup>/g and at the~~ average of 2.0±1.3 m<sup>2</sup>/g. ~~Obviously, the~~The absorption  
187 capability was higher for the ~~WISOC~~WIOC extract than the WSOC extract. This is thought to be

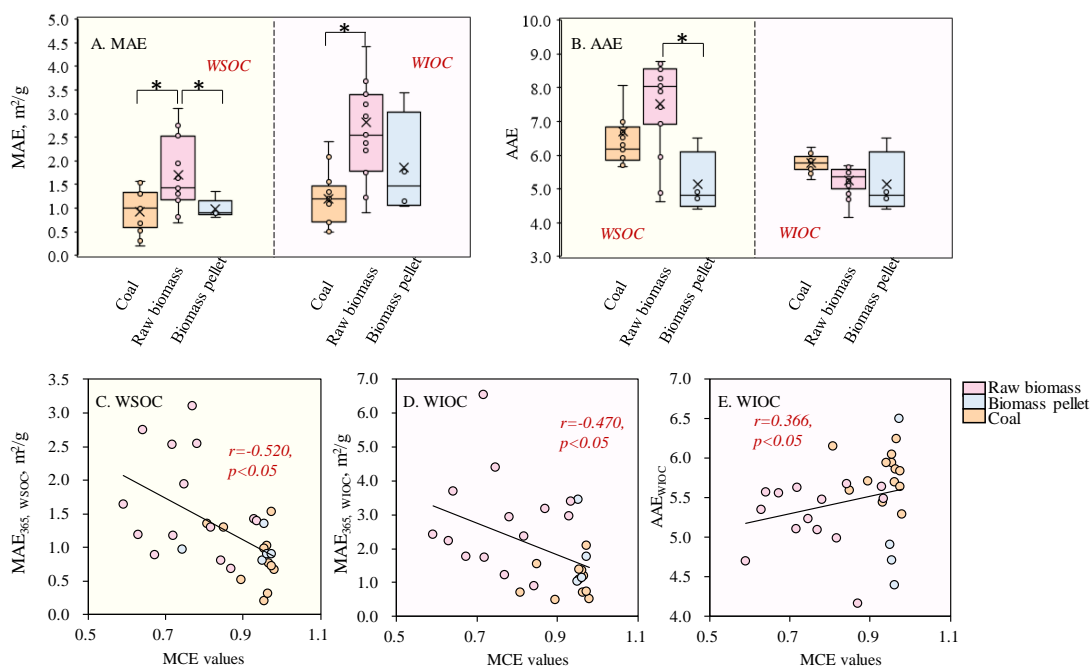
---

188 associated with distinct chemical compositions of light-absorbing organics. It was noted that the  
189 ~~WISOCWIOC~~ had higher MAE values compared to the WSOC, which may be explained by the  
190 more hydrophobic PAHs and quinones (Chen and Bond, 2010). The difference in MAE<sub>365, ~~WISOCWIOC~~</sub>  
191 among the different fuels was also statistically significant ( $p < 0.05$ ), as the value obtained from raw  
192 biomass burning ( $2.8 \pm 1.4 \text{ m}^2/\text{g}$ ) was significantly higher than that from coal combustion ( $1.2 \pm 0.6$   
193  $\text{m}^2/\text{g}$ ). ~~It was suggested that the MAE values of soluble OC including WSOC and WIOC~~ ~~The MAE~~  
194 ~~values of soluble OC~~ were dependent on the chemical composition of OC, that is, the chemical  
195 structure of the light-absorbing chromophores and the ratio of non-light-absorbing organics to the  
196 chromophore components (Cao et al., 2021). The higher MAE values of raw biomass combustion-  
197 derived aerosols might be caused by the stronger light absorption capability of chromophores or a  
198 higher ratio of chromophores. Our result was comparable to the published data, for example, the  
199 MAE<sub>365, WSOC</sub> was reported to average at  $1.37 \pm 0.23 \text{ m}^2/\text{g}$  for biomass burning emissions (Park and  
200 Yu, 2016). The correlation of MAE with the MCE was investigated. The variability in MAE values,  
201 for both WSOC and ~~WISOCWIOC~~, was observed to be negatively correlated with the MCE (or  
202 temperature as MCE was found to be positively correlated with the measured temperature in  
203 emission exhausts) when pooling all data together as seen in Fig. 1C and 1D. However, within each  
204 fuel group, there was no statistically significant correlation between the MAE and MCE values (Fig.  
205 S2). Some previous studies found that OC from wood pyrolysis under higher temperature conditions  
206 had stronger absorption capability (Chen and Bond, 2010; Saleh et al., 2014), but relatively higher  
207 mass absorption coefficient (MAC) values were also reported for the organic aerosol from wood  
208 combustion under the  $150^\circ\text{C} < T < 250^\circ\text{C}$  compared to emissions at a lower ( $T < 150^\circ\text{C}$ ) or higher  
209 ( $250^\circ\text{C} < T < 380^\circ\text{C}$ ) temperature condition (Rathod et al., 2017). Chen et al., (2010) reported that that  
210 absorption per mass ( $\alpha/\rho$ ) of methanol extracts increased with increased wood pyrolysis temperature,  
211 but such increase was nonlinear and varied in burning emissions of different fuel types or wood with

---

212 different sizes. Therefore, the negative correlations between MAE and MCE values when pooling  
213 all data together in Fig. 1 were from distinct absorption properties of emissions from different fuel  
214 types, rather than conditions like combustion temperature.

215 The AAE which indicates the wavelength dependence of light absorption is also an important  
216 parameter in climate models. The calculated AAE in the WSOC extract ( $AAE_{WSOC}$ ) ranged from  
217 3.8 to 11 with an average of  $6.9 \pm 1.5$ , and the difference in  $AAE_{WSOC}$  values among the different  
218 fuels was statistically significant ( $p < 0.05$ ) (Fig.1). The highest values were observed for the aerosols  
219 from raw biomass combustion of  $7.5 \pm 1.4$ , followed by coal smoke of  $6.7 \pm 1.5$  and biomass pellet  
220 smoke of  $5.6 \pm 1.2$ . The AAE values in the WISOCWIOC extract ( $AAE_{WISOCWIOC}$ ) were slightly  
221 lower than  $AAE_{WSOC}$ , which ranged from 4.2 to 6.5 with an average of  $5.5 \pm 0.5$ . The differences in  
222  $AAE_{WISOCWIOC}$  values among the different fuels were statistically insignificant ( $p > 0.05$ ), with  
223 averaged values of  $5.8 \pm 0.3$  for coal smoke,  $5.1 \pm 0.9$  for biomass pellet smoke, and  $5.2 \pm 0.4$  for raw  
224 biomass smoke. There was a weak positive correlation of  $AAE_{WISOCWIOC}$  between the MCE values  
225 ( $p < 0.05$ ). The filter-based analysis also showed that AAE values were positively correlated with  
226 MCE values, indicating that more BrC were produced under the smoldering phase compared with  
227 BC (Zhang et al., 2020). This study suggested that BrC in WIOC extract~~soluble BrC~~ was apt to be  
228 generated during the smoldering phase in comparison with the non-light-absorbing OC. The AAE  
229 values in soluble OC in this study were higher than 4 for all samples, confirming the contribution  
230 of BrC to aerosol absorptivity from source emission. The result of this study was comparable to the  
231 published literature. For example, it was reported that the  $AAE_{WSOC}$  was in the range of 8.6-15 from  
232 coal combustion-derived aerosols (Song et al., 2019), and 6.2-9.3 from biomass smoke (Park and  
233 Yu, 2016). The  $AAE_{WISOCWIOC}$  from wintertime urban aerosols were  $5.4 \pm 0.2$  in Xi'an and  $5.7 \pm 0.2$   
234 in Beijing (Huang et al., 2020).



235 **Fig. 1** MAE values at  $\lambda=365$  nm (A) and AAE values (B) from the source samples (\* represents  
 236  $p < 0.05$ ); Correlation between the MCE values with MAE<sub>365, WSOC</sub> values (C), MAE<sub>365, WIOC</sub>  
 237 values (D), and AAE<sub>WIOC</sub> values (E).

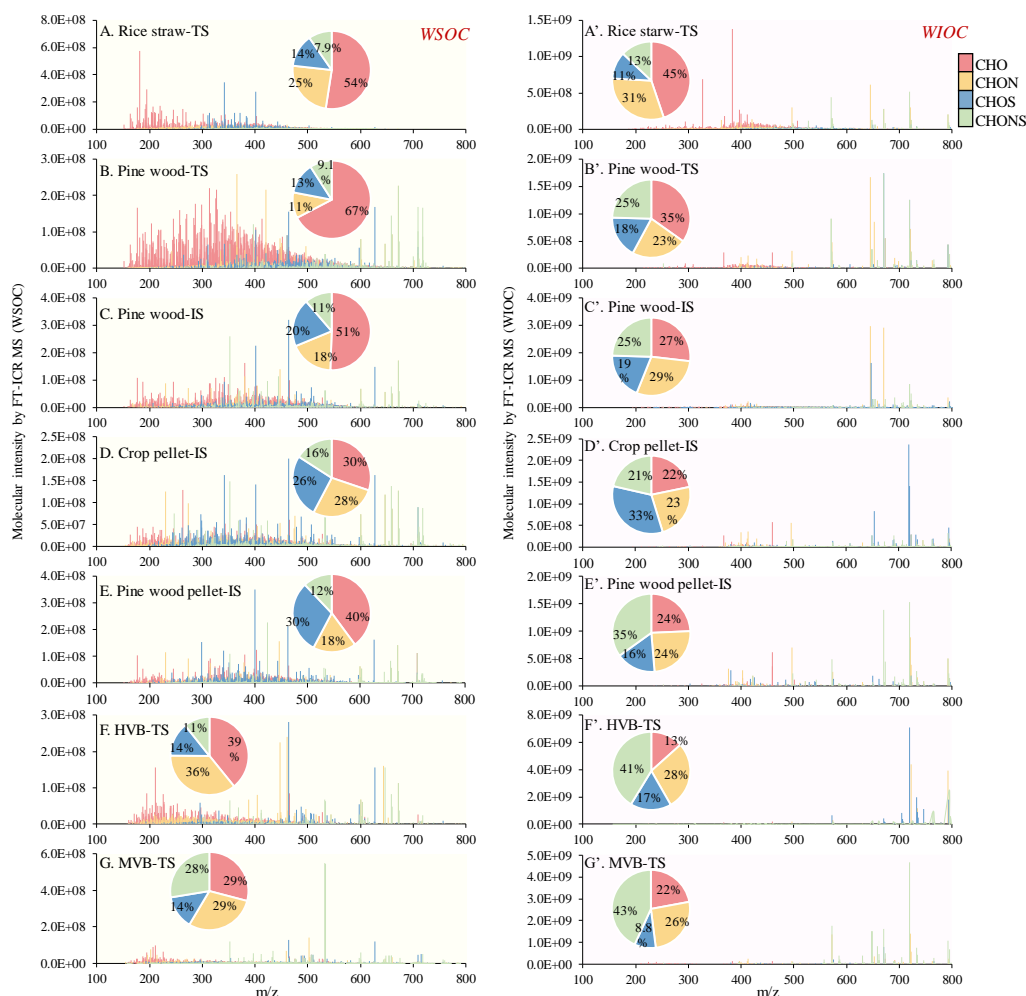
### 238 3.2 Molecular characteristics of WSOC and WIOC

239 The ESI-FT-ICR mass spectra of WSOC and WIOC samples are presented in Fig. 2.  
 240 Thousands of peaks were identified in the  $m/z$  range of 150-800, indicating a complex chemical  
 241 composition of aerosols from residential sources. Formulas detected in the raw biomass burning  
 242 aerosols were significantly higher than those in biomass pellet and coal smoke (Fig. S3), which  
 243 indicated a higher chemical complexity of raw biomass emissions. In addition, the combustion of  
 244 pine wood in the improved stove generated fewer compounds, which was 93% of ~~the peaks of~~  
 245 ~~that identified~~ in the traditional stove (Table S2). The likely less complexity might be due to higher  
 246 combustion efficiencies and temperature in the improved stove. Generally, higher levels of organic  
 247 aerosol mass would be emitted during less efficient fuel burning, resulting from prolonged  
 248 smoldering or incomplete burning (Holder et al., 2016). Our results suggested that corresponding

---

249 higher chemical complexity was also produced during the incomplete combustion in the traditional  
250 stove. The most intense ion peaks were distributed in the 200-500 m/z for WSOC, accounting for  
251 58-86% of the total intensity. Similar results were also found in residential coal combustion (Song  
252 et al., 2019), biomass burning (Song et al., 2018), and ambient aerosols (Wozniak et al., 2008).

253 The mass spectra of ~~WISOC~~WIOC ~~are~~are different from the WSOC, especially in aerosol  
254 emitted from coal combustion (Fig. 2). ~~WISOC~~WIOC contained more molecules with larger m/z  
255 values of 600-800 in range, which indicated that ~~WISOC~~WIOC extract had more compounds with  
256 higher molecular weight (MW) than the WSOC extract. According to the molecular formulas and  
257 the intensity of each negative ion, the average molecular formulas for the WSOC were obtained  
258 with C atom from 20 to 24, H (21-29), N (0.32-0.75), O (5.6-7.0), and S (0.28-0.51) in the WSOC  
259 extract. All aerosols from biomass burning, either raw or pelletized ones, had higher relative O atom  
260 contents than coal smoke, indicating a higher oxidation degree of biomass emissions. For the  
261 ~~WISOC~~WIOC, the average molecular formulas were assigned with 27-33 C, 26-35 H, 0.67-1.2 N,  
262 6.6-11 O, and 0.34-0.92 S. The coal combustion-derived aerosols had more C, N, and S atoms, but  
263 less H atom, compared with raw biomass. The combustion of biomass pellets is also assigned with  
264 relatively higher S elements. In addition, the ~~WISOC~~WIOC fraction had a higher relative atom  
265 content than the corresponding formulas of WSOC from the same source aerosol samples. These  
266 results indicated that in addition to the fuel type, extraction solvent also had an important impact on  
267 the elemental composition of extractable BrC.



268 **Fig. 2** Negative ESI FT-ICR mass spectra of WSOC (A-G) and ~~WSOC~~WIOC (A'-G') from the  
 269 seven aerosol samples. TS represents combustion in the traditional stove and IS represents  
 270 combustion in the improved stove. Different formula groups were color-coded. The pie charts  
 271 showed the relative intensities of different formula groups.

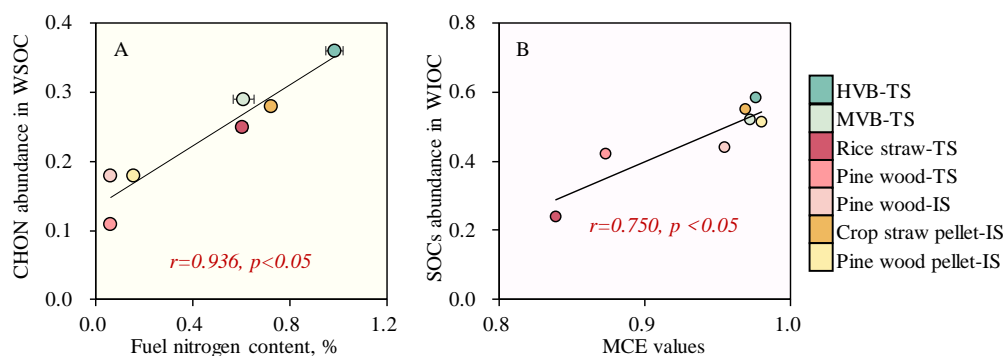
272 Molecular formulas identified by the FT-ICR-MS can be classified into 4 groups according to  
 273 the elemental composition, including CHO (containing only C, H, O), CHON (hereafter similarly),  
 274 CHOS, and CHONS. CHO was the most abundant group in the WSOC. The CHO group contributed  
 275 51-67% to the total intensity of aerosols from raw biomass burning, which were significantly higher  
 276 than those from biomass pellets (29-39%) and coal smoke (30-40%). The CHO compounds with  
 277 oxygen-containing functional groups (e.g., hydroxyl, carbonyl, carboxyl, or esters) have been  
 278 widely identified in both ambient aerosols (Jiang et al., 2021; Mo et al., 2022) and some source

---

279 samples (Tang et al., 2020). These compounds contributed a broad range of proportions, from 43%  
280 to 69% in residential biomass burning smoke (Tang et al., 2020), 9.7-48% in coal smoke (Song et  
281 al., 2019), and 20-39% in ambient aerosols (He et al., 2023) for the WSOC extract, which were  
282 comparable to ours. CHON compounds were also an important component in the aerosols,  
283 accounting for 29-36% ~~in-of~~ coal ~~smokes~~smoke, which ~~were~~-was significantly higher than biomass  
284 burning ~~smokes~~-smoke of 11-28%. One previous study reported that CHON species were more  
285 abundant in biomass burning smoke rather than ~~in the~~-coal combustion ones (Song et al., 2018).  
286 This high fraction of CHON compounds in coal ~~smokes~~-smoke might be caused by ~~the~~ higher  
287 nitrogen content of coals as seen in Table S1. A strongly significantly positive correlation was found  
288 between the fuel nitrogen content and CHON species percentage ( $r=0.936$ ,  $p<0.05$ ) (Fig. 3). Such  
289 dependence was also found in the emission factors (EFs) of NO<sub>x</sub> (~~NO<sub>x</sub> EFs~~) on fuel nitrogen content  
290 in our result (Fig. S4), as well as NO<sub>x</sub>, HCN, and NH<sub>3</sub> emissions reported by published ~~literatures~~  
291 literature (Hansson et al., 2004). Sulfur-containing compounds (SOCs; including CHOS and  
292 CHONS) abundance was lower than CHO and CHON group, accounting for only 22-42% (13-30%  
293 for CHOS and 7.9-28% for CHONS, respectively). The fractions of SOC<sub>s</sub> in the aerosols from coal  
294 combustion (25-42%) and biomass pellet burning (~42%) were comparable, but significantly higher  
295 than those from raw biomass (22-31%). The abundance of SOC<sub>s</sub> was not statistically correlated  
296 with fuel S content in the present study for pooled data. However, when fuel subgroups were  
297 considered, fuels (coal or raw biomass) with higher sulfur content had higher SOC<sub>s</sub> levels. Also,  
298 higher SOC<sub>s</sub> emission was found for pine wood combusted in the improved stove which have higher  
299 combustion efficiency than that in the traditional stove. These results suggested that except for fuel  
300 sulfur content, the fuel type and combustion efficiency would also influence the SOC<sub>s</sub> emissions.

301 In the ~~WISOC~~WIOC, the intensities of these four groups among different source samples were  
302 different from those in the WSOC. The CHO group accounted for 27-45% ~~of-in~~ raw biomass burning

303 aerosols, 22-24% in biomass pellet smokes, and 13-22% of coal smokes. On the contrary, the SOCs  
 304 abundance was significantly higher in WISOCWIOC, especially for the coals, accounting for 58%  
 305 for HVB<sub>7</sub> and 52% for MVB. A significantly positive correlation between the MCE values and SOCs  
 306 abundance in the WISOCWIOC extract was found ( $r=0.750$ ,  $p<0.05$ ) (Fig. 3), while no clear  
 307 association between fuel sulfur content and SOCs emissions was observed in the WISOCWIOC.  
 308 Combining the result from the WSOC extract, the strong dependence of SOCs emissions on the  
 309 combustion conditions was expected, while the fuel sulfur content had a slight influence. Notably,  
 310 the SOCs<sub>s</sub> abundance in aerosols from coal combustion was greatly higher than that in ambient  
 311 aerosols (Lin et al., 2012), indicating that residential non-desulfurized coal combustion might be an  
 312 important emitter of SOCs<sub>s</sub> in atmospheric samples. ~~Thus, t~~The CHON group emissions were  
 313 determined mainly by the fuel nitrogen content, while SOCs emissions were strongly related to the  
 314 combustion conditions (e.g., flaming phase). It should be noted that the results of our analysis based  
 315 on the current data without isotopic internal standard used were semi-quantitative, some  
 316 uncertainties must be addressed.



317 **Fig. 3** Correlation between fuel nitrogen contents and abundances of CHON in WSOC (A), and the  
 318 correlation between MCE values and the abundances of SOCs in WISOCWIOC (B). TS  
 319 represents combustion in the traditional stove and IS represents combustion in the  
 320 improved stove.



---

### 321 3.3 Detailed CHO/CHON/CHOS/CHONS group differences across fuel types

322 Van Krevelen (VK) diagrams which can provide a visual interpretation of complex mass  
323 spectra can qualitatively identify chemical composition profiles in mixtures (Lv et al., 2016). The  
324 classification criteria of the VK diagram are provided in Table S3 (Patriarca et al., 2018; Tang et al.,  
325 2020). Fig. S5 and S6 show the VK diagrams of WSOC and ~~WISOC~~WIOC. In both WSOC and  
326 WSOC extract, the carboxylic-rich alicyclic molecules (CRAM~~s~~-like) were the most abundant  
327 component, contributing to 53-69% in the WSOC extract and 37-56% in the ~~WISOC~~WIOC extract,  
328 respectively. The condensed aromatics were also an important component in source samples,  
329 accounting for 7.3-13% in the WSOC, and for a higher proportion of 8.6-44% in the ~~WISOC~~WIOC.  
330 This observation could be attributed to the hydrophobic property of condensed aromatic  
331 hydrocarbons, leading to a lower proportion in the highly polar WSOC. Among the identified  
332 formulas, 7.0-13% of total intensity in the WSOC and 3.6-17% in the ~~WISOC~~WIOC were the  
333 aliphatic/~~peptides like~~peptide-like compounds. Such fractions were comparable to unsaturated  
334 hydrocarbons with percentages of 3.9-15% in the WSOC and 2.0-11% in the ~~WISOC~~WIOC. The  
335 compounds including lipids-like species and highly oxygenated compounds (HOC) were in a  
336 relatively lower abundance, with less than 10% each in the source samples. The different fuels  
337 showed varied chemical composition characteristics. Coal combustion aerosols had lower H/C  
338 ratios than those in biomass burning aerosols, indicating higher unsaturated degrees (Table S2). As  
339 indicated by the VK diagrams, the coal combustion produced a notable number of condensed  
340 aromatics, contributing to 27%-44% ~~in~~of the ~~WISOC~~WIOC, which was significantly higher than  
341 ~~that~~ 8.6-21% in biomass burning emissions. The modified aromaticity index ( $AI_{mod,w}$ ) which is a  
342 measure of aromatic and condensed aromatic structure fractions, and ~~the double bonds equivalent~~  
343 (DBE) values which ~~is~~are used as a measure of the unsaturated level in a molecule were all higher  
344 for coal emissions compared to the biomass emissions.

345 Distinct compound profiles being identified by the VK diagram classification criteria are  
346 consistent with discrepancies in the four ~~(CHO/CHON/CHOS/CHONS)~~ groups  
347 (CHO/CHON/CHOS/CHONS). For the CHO group, the most intense compounds were CARMs  
348 compounds with fractions of 69-84% in the WSOC extract and higher fractions of 51-80% in the  
349 WISOCWIOC extract. It was observed that raw biomass would emit slightly more CRAMs (76-84%  
350 in the WSOC and 61-80% in the WISOCWIOC) than coal (69-73% in the WSOC and 62-69% in  
351 the WISOCWIOC) and biomass pellet (70-75% in the WSOC and 51-56% in the WISOCWIOC)  
352 combustion. The condensed aromatic compound was also a crucial component, accounting for 13-  
353 20% ~~of of~~ the WSOC and 19-27% of the WISOCWIOC ~~of from~~ coal emissions. These fractions  
354 were significantly higher than those found in raw biomass (4.5-10% in the WSOC, 7.9-10% in the  
355 WISOCWIOC) and biomass pellet (3.8-5.4% in the WSOC, and 11% in the WISOCWIOC) (Fig.  
356 4). The other components accounted for a small (less than 10% each) of the total CHO intensity.

357 It was reported that the CHON compounds with  $O/N \geq 3$  might be the organonitrates candidate  
358 and nitro-substituted compounds, attributing to the allocation of one nitro ( $\text{NO}_2$ ) or nitrooxy ( $\text{ONO}_2$ )  
359 group (Bianco et al., 2018). In this study, the relative content of  $\text{CHON}_{O/N \geq 3}$  compounds (concerning  
360 the overall CHON) in the biomass (raw and pellet ones) ranged between 71-82% and 85-91% for  
361 the WSOC and WISOCWIOC, which is distinctly lower than those found in coal smokes (86-90%  
362 for the WSOC, and 86-95% for the WISOCWIOC) (Table S4). Moreover, the  $\text{AI}_{\text{mod,w}}$  values for  
363 CHON compounds from coal combustion were higher than the biomass smokes for both WSOC  
364 and WISOCWIOC, as indicated by Table S2. It can thus be concluded that more CHON compounds  
365 with low aromaticity and a large amount of oxidized nitrogen functional groups were formed during  
366 the combustion of biomass fuels. Coal combustion emissions had more intense condensed aromatic  
367 compounds with ~~the a~~ percentage of 45-50% for the CHON group, which were significantly higher  
368 than those from raw biomass (4.5-37%) and biomass pellet burning (14-30%). This result confirmed

---

369 the conclusion that the CHON compounds produced from the combustion of coals were  
370 characterized by a relatively high aromaticity and a low degree of oxidation.

371 The O-rich CHOS fraction ( $O/S \geq 4$ ) accounted for 42-71% (concerning the overall CHON  
372 group) in the WSOC and 45-95% in the WISOCWIOC. O-rich CHOS fraction ( $O/S \geq 4$ ) content from  
373 coal (66-70% in the WSOC, and 78-98% in the WISOCWIOC) and biomass pellet (67-71% in the  
374 WSOC, 76-87% in the WISOCWIOC) were relatively higher than the raw biomass smoke (42-56%  
375 in the WSOC, and 32-57% in the WISOCWIOC), suggesting that most of the CHOS compounds in  
376 coal and pellet smoke can be potentially assigned with more bearing sulfate ( $-\text{OSO}_3\text{H}$ ) or sulfonate  
377 ( $-\text{SO}_3$ ) groups. Different from CHO and CHON groups, it was found that the CHOS group in the  
378 biomass burning aerosols had a much more intense condensed aromatic structure with ~~the a~~  
379 percentage of 14-33% in the WSOC and 2.5-19% in the WISOCWIOC, especially for raw biomass  
380 (WSOC: 22-33%, WISOCWIOC: 8.5-19%), than coal combustion (WSOC: 4.9-7.0%,  
381 WISOCWIOC: 2.5-7.0%). For the CHOS group in the WISOCWIOC extract, the unsaturated  
382 hydrocarbons were also an important component, accounting for 12-29% of raw biomass burning  
383 emissions, which were significantly higher than those in biomass pellet (6.9-11%) and coal (1.5-  
384 13%). These results indicated biomass burning emissions were characterized by higher unsaturation  
385 levels and aromaticity for the CHOS group than coal combustion.

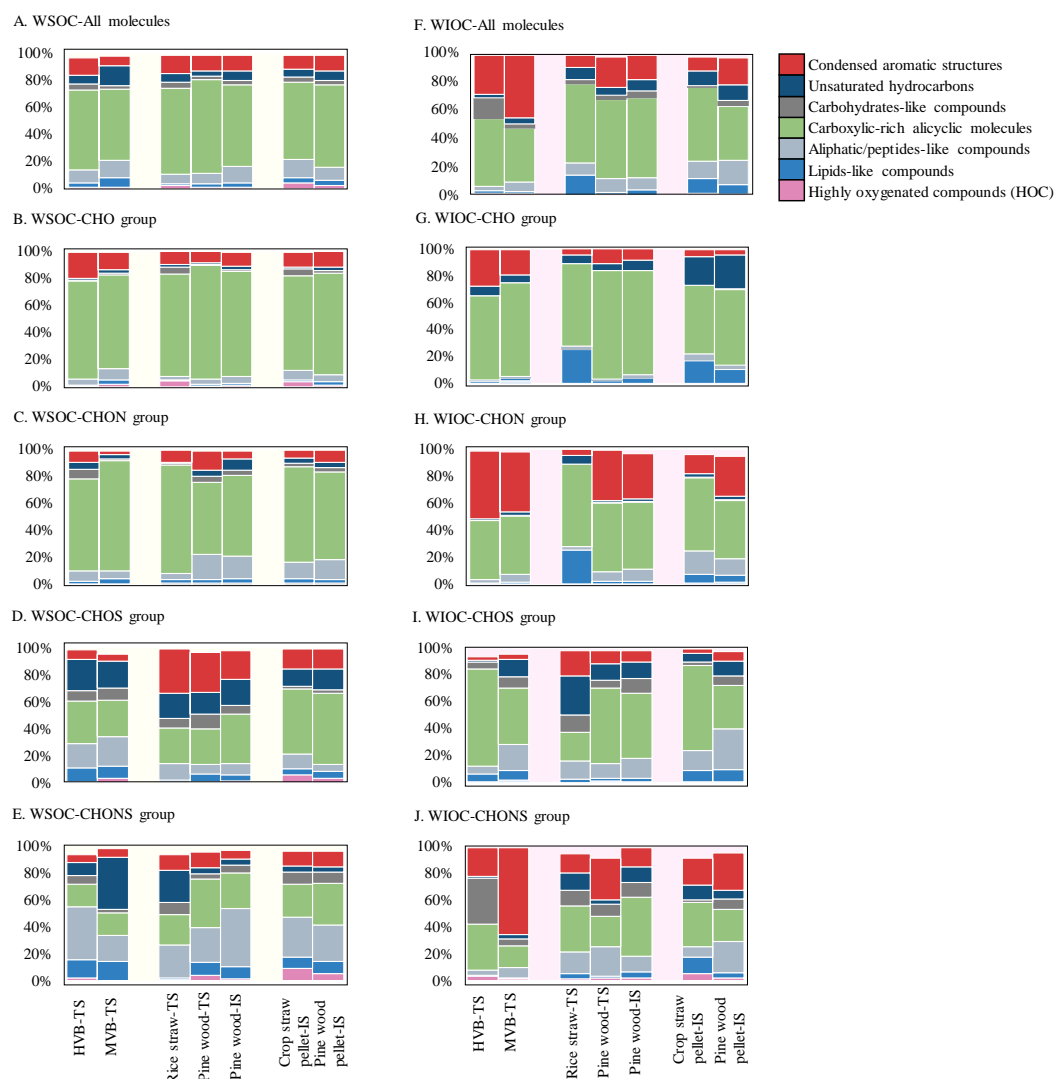
386 Nearly 34-85% of CHONS formulas have ~~a large number of many~~ O atoms ( $\geq 7$ ), indicating the  
387 existence of ~~the~~  $-\text{NO}_3$  group (Table S4). These CHONS compounds are probably nitrooxy-  
388 organosulfates (Song et al., 2019). The remaining compounds (15-66%) of the CHONS group had  
389 less than 7 atoms, implying that large amounts of CHONS compounds were assigned with reduced  
390 N (e.g., amide and nitrile, and heterocyclic aromatics). The condensed aromatic compounds  
391 identified by the VK diagram in the WISOCWIOC from coal combustion accounted for 22-64%,

---

392 which was relatively higher than those from biomass burning (14-31%), indicating a higher degree  
393 of aromaticity. This was consistent with the difference observed in the  $AI_{mod,w}$  values as seen in  
394 Table S2. The  $AI_{mod,w}$  of ~~WISOC~~WIOC in coal emissions were 0.38 for HVB and 0.60 for MVB,  
395 and the values were higher than the raw biomass (0.32-0.38) and biomass pellet (0.35-0.36),  
396 confirming a higher aromatic compounds content of coal smoke sample than biomass for CHONS  
397 group.

398 Therefore, the CHO, CHON, and CHONS groups generated from coal combustion were  
399 characterized by high unsaturated levels with more aromatic species, while CHOS groups had  
400 higher aromaticity degrees in biomass smoke aerosols. Aromatic compounds might be the strong  
401 BrC chromophores contributing to light absorption (Song et al., 2019). The difference in MAE  
402 between coal and biomass emissions and its association with the chemical components will be  
403 discussed in detail in section 3.5.

404



405 **Fig. 4** Each component abundance identified by VK diagram of WSOC (A: all molecules, B: CHO  
 406 group, C: CHON group, D: CHOS group, E: CHONS group) and ~~WSOC~~WIOC (F: all molecules,  
 407 G: CHO group, H: CHON group, I: CHOS group, J: CHONS group), the classification criteria  
 408 was provided in the Table S3.

### 409 3.4 Likely unique molecules of biomass and coal combustion

410 The unique molecules may be inferred from the Venn diagram of formulas as shown in Fig. S7.

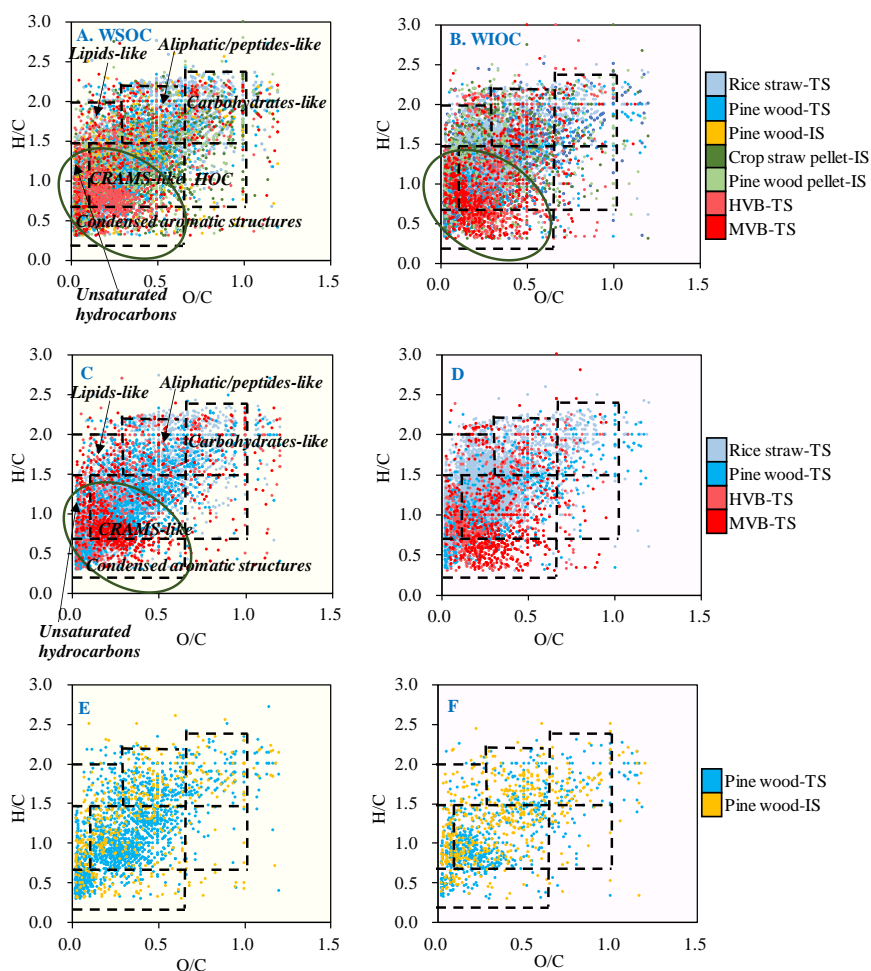
411 Among the observed wood compounds, 3039 and 1624 unique molecular formulas were detected in the  
 412 combustion of rice straw and pine wood in the traditional stove in the WSOC fractions, which was  
 413 significantly higher than those found. ~~These were significantly more than the unique formulas~~  
 414 ~~detected~~ in biomass pellet-improve stove ((638-696) and coal-traditional stove (570-734) ~~in the~~

---

415 ~~WSOC fractions. This~~, suggesting a notable difference between the emissions from raw biomass  
416 and coal, even when using the same stove. Interestingly, fewer unique peaks were observed for pine  
417 wood-improved stoves (533), indicating that using an improved stove for raw biomass could narrow  
418 the difference between coal and biomass emissions. A similar trend was also found in the  
419 ~~WISOCWIOC~~ fractions (Fig. S7). The CHONS group accounted for a significant portion of unique  
420 formulas in source samples, particularly in coal smokes, representing 51-52% in WSOC and 51-69%  
421 in ~~WISOCWIOC~~ extract. The important role of the CHONS group in unique emissions from coal  
422 combustion was also noted by Tang et al., (2020), who reported that CHO and CHON were the main  
423 components of unique molecular formulas of raw biomass burning emissions among the raw  
424 biomass burning, coal combustion and vehicle emissions, representing 88%-93%. This fraction was  
425 higher than our result of 33-77% in raw biomass and only 26-27% in biomass pellet. The distribution  
426 of the unique molecules further indicated substantial discrepancies among the fuels. Unique  
427 molecules in coal combustion-derived aerosols were in the region with lower H/C and O/C values  
428 compared with all other samples (Fig. 5) in both WSOC and ~~WISOCWIOC~~ extract, indicating a  
429 higher degree of unsaturation and lower level of oxidation. For example, it was observed that  
430 specific emissions from coal combustion were mainly composed of condensed aromatics (32-59%),  
431 followed by ~~CRAMsCRAMs~~ compounds (23-39%) in ~~WISOCWIOC~~ extract. However, only 4.3-  
432 9.7% condensed aromatics of the total unique emissions were observed for biomass burning, with  
433 ~~CRAMsCRAMs~~ being the main component (39-65%). As for different groups of CHO/CHON/  
434 CHONS, the condensed aromatic compound contents for all three groups in coal smoke aerosol  
435 (unique detected ones) were relatively higher than biomass. While CHOS group showed a different  
436 trend in that condensed aromatic compound contents of biomass smoke (unique detected ones) were  
437 relatively higher than coal smoke in WSOC extract and comparable to coal smoke in ~~WISOCWIOC~~  
438 extract. This finding highlighted the CHOS group's importance in distinguishing the aerosols from

439 the combustion of coals or biomass, helping conduct the source apportionment of aerosols.  
 440 Additionally, compared with the pine wood-improved stove emissions, most unique molecules in  
 441 aerosol from pine wood-traditional stove combustion were in the region with lower H/C and O/C  
 442 ratios (Fig. 5), which were identified mainly as CRAMS compounds. The emissions from  
 443 the improved stove were distributed in a wider range with fewer CRAMS compounds and  
 444 more aliphatic/peptides-like compounds observed. Unique molecules from biomass pellets  
 445 combusted in the improved stove distributed in the upper region of the VK diagram with higher H/C  
 446 values in WISOC extract, which indicated a lower unsaturated degree (Fig. S8).

447



448 **Fig. 5** Van Krevelen diagrams of WSOC (left) and WISOC (right) from the source samples.  
 449 TS represents combustion in the traditional stove and IS represents combustion in the improved  
 450 stove. Different color indicates unique formulas detected in each sample of solid fuel combustion.

---

451 A total of 484 molecular formulas were detected simultaneously in the seven aerosol samples  
452 in the WSOC extract and 306 in the WISOCWIOC extract. Among these commonly detected  
453 molecules, most of which were CHO compounds with the molecular numbers accounting for 60%  
454 and 73% in the WSOC and WISOCWIOC, respectively. CHON accounted for 31% of WSOC and  
455 19% of WISOCWIOC, while SOCs only occupied about 10%. As seen in Fig. S9, these CHO  
456 compounds were mainly composed of CRAMs-like compounds, ~~and~~ ~~and~~ several lipids-like and  
457 aliphatic/peptides-like compounds. Moreover, these compounds were relatively small molecular  
458 compounds assigned with 8-28 C atoms and 2-12 O atoms with DBE values of 2-17 for the WSOC  
459 extract. The relatively more C atom assigned with larger DBE values was observed for the CHO  
460 compounds in WISOCWIOC, which could be partially explained by that the overall CHO  
461 compounds in the WISOCWIOC extract had larger MW values with a high degree of unsaturation.  
462 In total, the CHON compounds were also CRAMs-like compounds, and almost none compounds  
463 were expected to be aromatics. CHOS and CHONS species had much fewer formulas, especially  
464 for CHONS, only accounting for 1.0% ~~in of~~ the commonly detected molecules in the WISOCWIOC.  
465 The unsaturated levels of commonly detected molecules in all seven source samples were relatively  
466 low. For example, the condensed aromatic compounds accounted for 6.5-9.3% and 3.3-4.1% of the  
467 total intensity for coal smoke and biomass smoke in the WSOC, respectively, as well as 0.38-8.3%  
468 and 18-21% in the WISOCWIOC extract. Different from the CHO, CHON, and CHONS groups,  
469 high percentages of condensed aromatic compounds were found in the CHOS group (commonly  
470 detected ones) from raw biomass burning aerosols with a range of 6.6-51% in the WSOC and 12-  
471 46% in the WISOCWIOC extract. These fractions were significantly higher than those from coal  
472 smokes of 4.1-4.9% in the WSOC and 8.8-25% in the WISOCWIOC extract. Combining the finding  
473 that the CHOS group in biomass smokes had a higher aromaticity degree in both WSOC and  
474 WISOCWIOC extract. However, the unique molecules in WISOCWIOC extract did not follow this



---

475 trend. It was thus speculated that the higher aromaticity degree of the CHOS group in biomass  
476 smokes was attributed to the intensity variation of these simultaneously detected compounds, rather  
477 than the unique emission from a special source for the WISOCWIOC extract.

478 To explore the potential influence of fuel properties and combustion conditions on chemical  
479 composition, the major factors such as fuel moisture,  $V_{daf}$ , and parameters reflecting combustion  
480 conditions including MCE, and EC/OC ratios were assessed. The linear correlation analysis was  
481 applied to estimate the effect of these factors on each molecular intensity (commonly detected ones)  
482 (Fig.S10 and S11). The aliphatic compounds (including lipids-like, aliphatic/peptides-like, and  
483 carbohydrates-like compounds) were negatively correlated with the fuel moisture and positively  
484 correlated with  $V_{daf}$  and EC/OC ratios. Fuel moisture has been recognized as an important factor  
485 influencing pollutant formation, but the influence is usually very complicated. The observed  
486 relationship between fuel water content and pollutant EFs varies largely among studies, which may  
487 be attributed to factors such as different water contents, pollutant types, and interactions among  
488 other influencing factors. Fuels with high moisture levels may have high emissions, as extra energy  
489 is needed to vaporize water during the burning process; however, a decrease in combustion  
490 temperatures under very high-water content conditions may slow the pollutant formation rate and  
491 consequently lower emissions. Higher EC/OC ratios and larger MCE values tend to be associated  
492 with stronger flaming conditions. The results suggested that the aliphatic compounds were apt to be  
493 produced during the period of the flaming phase with higher combustion temperature. This result  
494 could partially explain that aliphatic/peptides-like compounds would be apt to be produced in the  
495 improved stove rather than the traditional stove. In comparison, the emissions of CRAMs-like  
496 compounds which are the most abundant species were decreased with the increased MCE and  
497 EC/OC values, indicating that CARMs-like compounds were generated under the smoking phase.  
498 No significant correlations of aromatics, unsaturated hydrocarbons, and HOCs were observed with

---

499 these parameters, resulting from their small proportion in commonly detected molecules. It is worth  
500 noting that there may be significant differences, even for the same fuel, in chemical composition  
501 depending on other factors such as stove type and combustion conditions. The interactions among  
502 these factors make it difficult to assess their influence. It was found that only around 50% of  
503 identified molecules were overlapped emissions for pine wood combusted in the traditional stove  
504 and in the improved stove, suggesting the importance of the stove used. A smaller fraction of 25-  
505 30% molecules were observed compared to the pine wood emissions with coals combusted in the  
506 same stove, which suggested that the influence of varied fuels on chemical composition could  
507 surpass the differences caused by different stoves. Our previous studies have revealed that fuel type  
508 was the most important factor influencing the MAE values (Zhang et al., 2021b) and BrC EFs  
509 (Zhang et al., 2021a). The present study highlighted the dominant effect of fuel type on the chemical  
510 composition of soluble OC, providing a theoretical basis for source appointment based on molecular  
511 composition. Moreover, the combustion conditions would have a significant effect on the molecular  
512 intensity, resulting in differences in MAE eventually as indicated in section 3.1.

### 513 3.5 The correlation of light absorption properties with molecular compositions

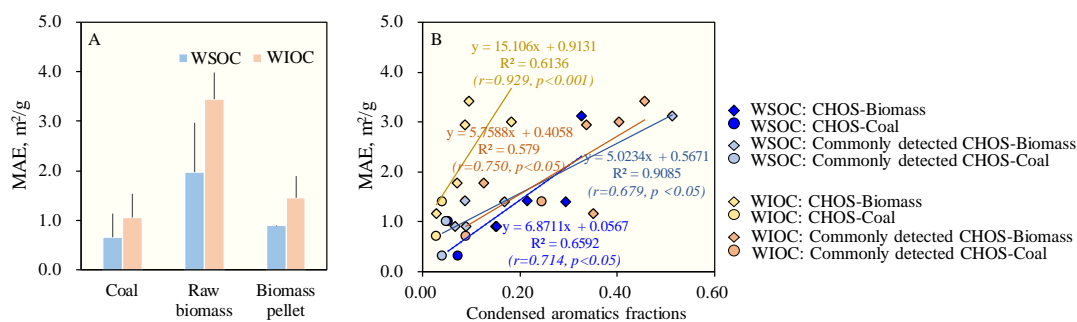
514 Here we specifically ~~look into~~investigate the variability in optical characteristics among the  
515 different fuels attributed to ~~its~~their chemical compositions. No significant correlations were  
516 observed between the AAE values of soluble OC and the molecular composition, indicating that  
517 AAE could be influenced by many factors. The MAE may be influenced by the degree of oxidation  
518 and unsaturation degree (Mo et al., 2017) (Tang et al., 2020), however, there was no significant  
519 correlation found between the MAE values and O/C values in the present source samples, implying  
520 that the BrC light absorption ability might not be directly affected by its oxidation degree.

521 The MAE<sub>365, -wsoc</sub> values were significantly positively correlated with the DBE values

---

522 ( $r=0.786, p<0.05$ ) and the MW values ( $r=0.750, p<0.05$ ) (Fig. S12), indicating that unsaturation and  
523 MW played a crucial role in the light absorption capability of the source samples. In the above  
524 discussion, we have noticed that the CHOS group in biomass was characterized by a higher degree  
525 of aromaticity than coal smoke aerosol, while the CHO, CHON, and CHONS ~~group-groups~~ have a  
526 higher aromatic degree in the coal emissions. A significantly positive correlation ( $r=0.714, p<0.05$ )  
527 was observed between ~~MAE<sub>365, wSOC</sub>~~MAE<sub>365, wSOC</sub> values, and the condensed aromatics percentages  
528 from the CHOS group (Fig. 6), indicating that aromatics in the CHOS group contributed to the high  
529 light absorption ability of biomass smokes.

530 For the ~~wSOCwIOC~~wSOCwIOC extract, no significant correlation was found between the MAE<sub>365, wIOC</sub>  
531 ~~MAE<sub>365, wSOC</sub>~~MAE<sub>365, wSOC</sub> values with MW or DBE values, which might be explained by much different  
532 chemical composition for insoluble compounds compared with soluble parts. Although the coal  
533 combustion emitted much more aromatic compounds with higher DBE values for the ~~wSOCwIOC~~wSOCwIOC,  
534 the MAE values were not significantly higher. The significantly positive correlation ( $r=0.929,$   
535  $p<0.05$ ) between MAE<sub>365, wSOCwIOC</sub> values, and the CHOS condensed aromatics percentages  
536 confirmed the importance of CHOS aromatics in determining the light absorption capability from  
537 source samples. As mentioned in Section 3.4, the higher aromaticity degree of the CHOS group in  
538 biomass smoke was largely due to the intensity variation of these commonly detected compounds  
539 in all source samples. Further analysis revealed that MAE<sub>365, wSOCwIOC</sub> values were positively  
540 correlated ( $r=0.750, p<0.05$ ) with the CHOS condensed aromatics fractions which were the fraction  
541 simultaneously detected in all samples. These results indicated that the light absorption capability  
542 of source aerosols may be due to the higher abundance of some CHOS aromatic compounds  
543 commonly emitted from both coal and biomass, rather than the unique tracers.



544 **Fig. 6** MAE values at  $\lambda=365$  nm (A) and correlations between MAE values and condensed aromatics  
 545 fractions in CHOS and in commonly detected CHOS (B) from the source samples

#### 546 4. Conclusion and implication

547 The  $MAE_{365, WSOC}$  ranged from 0.21 to 3.1 m<sup>2</sup>/g with an average of 1.3±0.7 m<sup>2</sup>/g. The  $MAE_{365, WIOC}$   
 548 was found to be higher with an average of 2.0±1.3 m<sup>2</sup>/g. There were significant  
 549 differences ( $p < 0.05$ ) observed among the different fuels for both  $MAE_{365, WSOC}$  and  
 550  $MAE_{365, WIOC}$ , as raw biomass burning combustion had significantly higher values than the  
 551 coal combustion. The  $AAE_{WSOC}$  ranged from 3.8 to 11 with an average of 6.9±1.5. The  
 552  $AAE_{WIOC}$  was slightly lower than  $AAE_{WSOC}$ , which ranged from 4.2 to 6.5 with an average of  
 553 5.5±0.5. Thousands of peaks were identified in the m/z range of 150-800, indicating a complex  
 554 chemical composition of aerosols from residential sources. CHO group was the most abundant  
 555 component in the WSOC extracts and the contribution of CHO compounds to the total intensity in  
 556 aerosols from raw biomass burning was significantly higher than those from biomass pellets and  
 557 coal smoke. On the other hand, WIOC extract contained more SOCs, especially in the coal  
 558 combustion aerosol. Notably, CHON compounds were more abundant in the coal combustion  
 559 emissions, which was due to the higher fuel N content of coals ( $r = 0.936, p < 0.05$ ). The SOCs  
 560 emissions were more predominant during flaming phases, with a positive correlation between SOCs  
 561 abundance with the MCE values ( $r = 0.750, p < 0.05$ ). The CHO, CHON, and CHONS groups  
 562 generated from coal combustion were characterized by high unsaturated levels with more aromatic

---

563 species, while CHOS groups had higher aromaticity degrees in biomass smoke aerosols. It was  
564 found that MAE values were positively correlated with the CHOS condensed aromatics proportion  
565 for both WSOC ( $r=0.714$ ,  $p<0.05$ ) and ~~WISOC~~WIOC extract ( $r=0.929$ ,  $p<0.001$ ). These results  
566 indicated that higher CHOS condense aromatics abundance in biomass burning aerosols could partly  
567 explain the higher MAE values of raw biomass smoke. Further analysis showed a positive  
568 correlation of MAE with the CHOS condensed aromatics fractions which were the fractions  
569 simultaneously detected in all samples. These results indicated that the light absorption capability  
570 of source aerosols may be due to the higher abundance of some CHOS aromatic compounds  
571 commonly emitted from both coal and biomass burning, rather than the unique tracers. The unique  
572 formulas of coal combustion aerosols were in the lower H/C and O/C regions with higher  
573 unsaturated compounds in the VK diagram. This work is potentially applicable to the source  
574 appointment based on the molecular characteristics and to future studies developing more scientific  
575 control measures by focusing on one major component (e.g., CHOS condensed aromatics) of light  
576 absorption aerosols.

577 There are still some questions that need to be investigated in the future study. First, the study on  
578 BrC composition in this research used dissolved OC as a substitute. However, this substitute cannot  
579 fully represent BrC emissions. Both WSOC and ~~WISOC~~WIOC contain some non-light-absorbing  
580 components, and the proportion of these components is unknown, making it difficult to measure the  
581 representativeness of extractable OC for BrC. Additionally, the lack of study about the emissions  
582 characteristics under controlled combustion conditions limits the obtained results. Controlled  
583 experiments including flaming or smoldering burns, airflow, and combustion temperature are  
584 needed in future work. Third, fresh burning-derived OC released into the atmosphere can undergo  
585 various aging reactions such as photochemical degradation. These reactions can significantly alter  
586 the light absorptivity and chemical properties of BrC components. It is essential to consider the

---

587 optical properties and lifetimes of organic compounds emitted from solid fuel combustion in climate  
588 models.

589 **Data availability.**

590 Data are available by contacting the corresponding authors

591 **Supplement**

592 The following information is in the appendix and available via the Internet:

593 Data processing in the ESI FT-ICR MS; fuel properties of coal and biomass fuels tested;  
594 number of formulas in each group, values of elemental ratios, MW, and DBE values in the WSOC  
595 and WISCO for each source type; Stoichiometric ranges of VK classes; Correlation between fuel N  
596 and emission factors of NO<sub>x</sub>; the VK diagrams of WSOC and ~~WISOC~~WIOC for different source  
597 samples; and correlations between the VK plots of WSOC/~~WISOC~~WIOC and fuel properties or  
598 combustion conditions.

599 **Author contributions**

600 LZ, GS, and ST designed the experiment. LZ and JL prepared the filters used. LZ, YL, XL and  
601 ZL conducted the sample collection. LZ and JL performed the data analysis. LZ wrote the paper.  
602 GS, and ST reviewed and commented on the paper.

603 **Competing interests**

604 The authors declare that they have no conflict of interest.

605 **Acknowledgment**

606 Funding for this study was partly from the National Natural Science Foundation of China  
607 (42077328, and 41922057). The authors greatly appreciated the valuable help in data analysis by

---

608 Prof. Jianzhong Song from CAS.

609 **Financial support**

610 This research has been supported by the National Natural Science Foundation of China  
611 (42077328, and 41922057)

612 **References**

613 Bianco, A., Deguillaume, L., Vaitilingom, M., Nicol, E., Baray, J.L., Chaumerliac, N., and  
614 Bridoux, M.: Molecular Characterization of Cloud Water Samples Collected at the Puy de Dome  
615 (France) by Fourier Transform Ion Cyclotron Resonance Mass Spectrometry, *Environ. Sci. Technol.*,  
616 52, 10275-10285, <https://doi.org/10.1021/acs.est.8b01964>, 2018.

617 Bond, T. C.: Spectral dependence of visible light absorption by carbonaceous particles emitted  
618 from coal combustion, *Geophys. Res. Lett.*, 28, 4075-4078, <https://doi.org/10.1029/2001GL013652>,  
619 2001.

620 Bond, T. C. and Bergstrom, R. W.: Light absorption by carbonaceous particles: An investigative  
621 review, *Aerosol Sci. Technol.*, 40, 27-67, <https://doi.org/10.1080/02786820500421521>, 2006.

622 Brege, M., Paglione, M., Gilardoni, S., Decesari, S., Facchini, M. C., and Mazzoleni, L. R.:  
623 Molecular insights on aging and aqueous-phase processing from ambient biomass burning  
624 emissions-influenced Po Valley fog and aerosol, *Atmos. Chem. Phys.*, 18, 13197-13214,  
625 <https://doi.org/10.5194/acp-18-13197-2018>, 2018.

626 Burling, I. R., Yokelson, R. J., Griffith, D. W. T., Johnson, T. J., Veres, P., Roberts, J. M.,  
627 Warneke, C., Urbanski, S. P., Reardon, J., Weise, D. R., Hao, W. M., and de Gouw, J.: Laboratory  
628 measurements of trace gas emissions from biomass burning of fuel types from the southeastern and  
629 southwestern United States, *Atmos. Chem. Phys.*, 10, <https://doi.org/10.5194/acp-10-11115-2010>,  
630 2010.

631 Cao, T., Li, M., Zou, C., Fan, X., Song, J., Jia, W., Yu, C., Yu, Z., and Peng, P.: Chemical  
632 composition, optical properties, and oxidative potential of water- and methanol-soluble organic  
633 compounds emitted from the combustion of biomass materials and coal, *Atmos. Chem. Phys.*, 21,  
634 13187-13205, <https://doi.org/10.5194/acp-21-13187-2021>, 2021.

635 Chen, Y. and Bond, T. C.: Light absorption by organic carbon from wood combustion, *Atmos.*  
636 *Chem. Phys.*, 10, 1773-1787, <https://doi.org/10.5194/acp-10-1773-2010>, 2010.

637 Du, Z., He, K., Cheng, Y., Duan, F., Ma, Y., Liu, J., Zhang, X., Zheng, M., and Weber, R.: A  
638 yearlong study of water-soluble organic carbon in Beijing II: Light absorption properties, *Atmos.*  
639 *Environ.*, 89, 235-241, <https://doi.org/10.1016/j.atmosenv.2014.02.022>, 2014.

640 Fan, X., Li, M., Cao, T., Cheng, C., Li, F., Xie, Y., Wei, S., Song, J., and Peng, P. a.: Optical  
641 properties and oxidative potential of water-and alkaline-soluble brown carbon in smoke particles  
642 emitted from laboratory simulated biomass burning, *Atmos. Environ.*, 194, 48-57,  
643 <https://doi.org/10.1016/j.atmosenv.2018.09.025>, 2018.

644 Feng, Y., Ramanathan, V., and Kotamarthi, V. R.: Brown carbon: a significant atmospheric  
645 absorber of solar radiation? *Atmos. Chem. Phys.*, 13, 8607-8621, <https://doi.org/10.5194/acp-13-8607-2013>, 2013.

647 Hansson, K. M., Samuelsson, J., Tullin, C., and Amand, L. E.: Formation of HNCO, HCN, and  
648 NH<sub>3</sub> from the pyrolysis of bark and nitrogen-containing model compounds, *Combust. Flame*, 137,

- 649 265-277, <https://doi.org/10.1016/j.combustflame.2004.01.005>, 2004.
- 650 He, T., Wu, Y., Wang, D., Cai, J., Song, J., Yu, Z., Zeng, X., and Peng, P. a.: Molecular  
651 compositions and optical properties of water-soluble brown carbon during the autumn and winter in  
652 Guangzhou, China, *Atmos. Environ.*, 296, <https://doi.org/10.1016/j.atmosenv.2022.119573>, 2023.
- 653 Holder, A. L., Hagler, G. S. W., Aurell, J., Hays, M. D., and Gullett, B. K.: Particulate matter  
654 and black carbon optical properties and emission factors from prescribed fires in the southeastern  
655 United States, *J. Geophys. Res.: Atmos.*, 121, 3465-3483, <https://doi.org/10.1002/2015JD024321>,  
656 2016.
- 657 Huang, R.J., Yang, L., Cao, J., Chen, Y., Chen, Q., Li, Y., Duan, J., Zhu, C., Dai, W., Wang, K.,  
658 Lin, C., Ni, H., Corbin, J. C., Wu, Y., Zhang, R., Tie, X., Hoffmann, T., O'Dowd, C., and Dusek, U.:  
659 Brown Carbon Aerosol in Urban Xi'an, Northwest China: The Composition and Light Absorption  
660 Properties, *Environ. Sci. Technol.*, 52, 6825-6833, <https://doi.org/10.1021/acs.est.8b02386>, 2018.
- 661 Huang, R.J., Yang, L., Shen, J., Yuan, W., Gong, Y., Guo, J., Cao, W., Duan, J., Ni, H., Zhu, C.,  
662 Dai, W., Li, Y., Chen, Y., Chen, Q., Wu, Y., Zhang, R., Dusek, U., O'Dowd, C., and Hoffmann, T.:  
663 Water-Insoluble Organics Dominate Brown Carbon in Wintertime Urban Aerosol of China:  
664 Chemical Characteristics and Optical Properties, *Environ. Sci. Technol.*, 54, 7836-7847,  
665 <https://doi.org/10.1021/acs.est.0c01149>, 2020.
- 666 Huo, Y., Li, M., Jiang, M., and Qi, W.: Light absorption properties of HULIS in primary  
667 particulate matter produced by crop straw combustion under different moisture contents and  
668 stacking modes, *Atmos. Environ.*, 191, 490-499, <https://doi.org/10.1016/j.atmosenv.2018.08.038>,  
669 2018.
- 670 Jen, C. N., Hatch, L. E., Selimovic, V., Yokelson, R. J., Weber, R., Fernandez, A. E., Kreisberg,  
671 N. M., Barsanti, K. C., and Goldstein, A. H.: Speciated and total emission factors of particulate  
672 organics from burning western US wildland fuels and their dependence on combustion efficiency,  
673 *Atmos. Chem. Phys.*, 19, 1013-1026, <https://doi.org/10.5194/acp-19-1013-2019>, 2019.
- 674 Jiang, B., Kuang, B. Y., Liang, Y., Zhang, J., Huang, X. H. H., Xu, C., Yu, J. Z., and Shi, Q.:  
675 Molecular composition of urban organic aerosols on clear and hazy days in Beijing: a comparative  
676 study using FT-ICR MS, *Environ. Chem.*, 13, 888-901, <https://doi.org/10.1071/EN15230>, 2016.
- 677 Jiang, H., Li, J., Sun, R., Tian, C., Tang, J., Jiang, B., Liao, Y., Chen, C.-E., and Zhang, G.:  
678 Molecular Dynamics and Light Absorption Properties of Atmospheric Dissolved Organic Matter,  
679 *Environ. Sci. Technol.*, 55, 10268-10279, <https://doi.org/10.1021/acs.est.1c01770>, 2021.
- 680 Jo, D. S., Park, R. J., Lee, S., Kim, S.-W., and Zhang, X.: A global simulation of brown carbon:  
681 implications for photochemistry and direct radiative effect, *Atmos. Chem. Phys.*, 16, 3413-3432,  
682 <https://doi.org/10.5194/acp-16-3413-2016>, 2016.
- 683 Laskin, A., Laskin, J., and Nizkorodov, S. A.: Chemistry of Atmospheric Brown Carbon, *Chem.*  
684 *Rev.*, 115, 4335-4382, <https://doi.org/10.1021/cr5006167>, 2015.
- 685 Laskin, A., Smith, J. S., and Laskin, J.: Molecular Characterization of Nitrogen-Containing  
686 Organic Compounds in Biomass Burning Aerosols Using High-Resolution Mass Spectrometry,  
687 *Environ. Sci. Technol.*, 43, 3764-3771, <https://doi.org/10.1021/es803456n>, 2009.
- 688 Li, J., Zhang, Q., Wang, G., Li, J., Wu, C., Liu, L., Wang, J., Jiang, W., Li, L., Ho, K. F., and  
689 Cao, J.: Optical properties and molecular compositions of water-soluble and water-insoluble brown  
690 carbon (BrC) aerosols in northwest China, *Atmos. Chem. Phys.*, 20, 4889-4904,  
691 <https://doi.org/10.5194/acp-20-4889-2020>, 2020.
- 692 Li, M., Fan, X., Zhu, M., Zou, C., Song, J., Wei, S., Jia, W., and Peng, P. a.: Abundance and  
693 Light Absorption Properties of Brown Carbon Emitted from Residential Coal Combustion in China,  
694 *Environ. Sci. Technol.*, 53, 595-603, <https://doi.org/10.1021/acs.est.8b05630>, 2019.
- 695 Lin, P., Rincon, A. G., Kalberer, M., and Yu, J. Z.: Elemental Composition of HULIS in the



---

696 Pearl River Delta Region, China: Results Inferred from Positive and Negative Electrospray High  
697 Resolution Mass Spectrometric Data, *Environ. Sci. Technol.*, 46, 7454-7462,  
698 <https://doi.org/10.1021/es300285d>, 2012.

699 Lv, J., Zhang, S., Wang, S., Luo, L., Cao, D., and Christie, P.: Molecular-Scale Investigation  
700 with ESI-FT-ICR-MS on Fractionation of Dissolved Organic Matter Induced by Adsorption on Iron  
701 Oxyhydroxides, *Environ. Sci. Technol.*, 50, 2328-2336, <https://doi.org/10.1021/acs.est.5b04996>,  
702 2016.

703 McMeeking, G. R., Kreidenweis, S. M., Baker, S., Carrico, C. M., Chow, J. C., Collett, J. L.,  
704 Jr., Hao, W. M., Holden, A. S., Kirchstetter, T. W., Malm, W. C., Moosmueller, H., Sullivan, A. P.,  
705 and Wold, C. E.: Emissions of trace gases and aerosols during the open combustion of biomass in  
706 the laboratory, *J. Geophys. Res.: Atmos.*, 114, <https://doi.org/10.1029/2009JD011836>, 2009.

707 Mo, Y., Li, J., Liu, J., Zhong, G., Cheng, Z., Tian, C., Chen, Y., and Zhang, G.: The influence  
708 of solvent and pH on determination of the light absorption properties of water-soluble brown carbon,  
709 *Atmos. Environ.*, 161, 90-98, <https://doi.org/10.1016/j.atmosenv.2017.04.037>, 2017.

710 Mo, Y., Zhong, G., Li, J., Liu, X., Jiang, H., Tang, J., Jiang, B., Liao, Y., Cheng, Z., and Zhang,  
711 G.: The Sources, Molecular Compositions, and Light Absorption Properties of Water-Soluble  
712 Organic Carbon in Marine Aerosols From South China Sea to the Eastern Indian Ocean, *J. Geophys.*  
713 *Res.: Atmos.*, 127, <https://doi.org/10.1029/2021JD036168>, 2022.

714 Olson, M. R., Garcia, M. V., Robinson, M. A., Van Rooy, P., Dietenberger, M. A., Bergin, M.,  
715 and Schauer, J. J.: Investigation of black and brown carbon multiple-wavelength-dependent light  
716 absorption from biomass and fossil fuel combustion source emissions, *J. Geophys. Res.: Atmos.*,  
717 120, 6682-6697, <https://doi.org/10.1002/2014JD022970>, 2015.

718 Park, S. S. and Yu, J.: Chemical and light absorption properties of humic-like substances from  
719 biomass burning emissions under controlled combustion experiments, *Atmos. Environ.*, 136, 114-  
720 122, <https://doi.org/10.1016/j.atmosenv.2016.04.022>, 2016.

721 Patriarca, C., Bergquist, J., Sjoberg, P. J. R., Tranvik, L., and Hawkes, J. A.: Online HPLC-  
722 ESI-HRMS Method for the Analysis and Comparison of Different Dissolved Organic Matter  
723 Samples, *Environ. Sci. Technol.*, 52, 2091-2099, <https://doi.org/10.1021/acs.est.7b04508>, 2018.

724 Pokhrel, R. P., Wagner, N. L., Langridge, J. M., Lack, D. A., Jayarathne, T., Stone, E. A.,  
725 Stockwell, C. E., Yokelson, R. J., and Murphy, S. M.: Parameterization of single-scattering albedo  
726 (SSA) and absorption Angstrom exponent (AAE) with EC / OC for aerosol emissions from biomass  
727 burning, *Atmos. Chem. Phys.*, 16, 9549-9561, [10.5194/acp-16-9549-2016](https://doi.org/10.5194/acp-16-9549-2016), 2016.

728 Rathod, T., Sahu, S. K., Tiwari, M., Yousaf, A., Bhangare, R. C., and Pandit, G. G.: Light  
729 Absorbing Properties of Brown Carbon Generated from Pyrolytic Combustion of Household  
730 Biofuels, *Aerosol Air Qual. Res.*, 17, 108-116, [10.4209/aaqr.2015.11.0639](https://doi.org/10.4209/aaqr.2015.11.0639), 2017.

731 Reisen, F., Meyer, C. P., Weston, C. J., and Volkova, L.: Ground-Based Field Measurements of  
732 PM2.5 Emission Factors From Flaming and Smoldering Combustion in Eucalypt Forests, *J.*  
733 *Geophys. Res.: Atmos.*, 123, 8301-8314, <https://doi.org/10.1029/2018JD028488>, 2018.

734 Ren, Q. and Zhao, C.: Evolution of fuel-N in gas phase during biomass pyrolysis, *Renewable*  
735 *Sustainable Energy Rev.*, 50, 408-418, <https://doi.org/10.1016/j.rser.2015.05.043>, 2015.

736 Saleh, R., Robinson, E. S., Tkacik, D. S., Ahern, A. T., Liu, S., Aiken, A. C., Sullivan, R. C.,  
737 Presto, A. A., Dubey, M. K., Yokelson, R. J., Donahue, N. M., and Robinson, A. L.: Brownness of  
738 organics in aerosols from biomass burning linked to their black carbon content, *Nat. Geosci.*, 7, 647-  
739 650, [10.1038/ngeo2220](https://doi.org/10.1038/ngeo2220), 2014.

740 Song, J., Li, M., Jiang, B., Wei, S., Fan, X., and Peng, P. a.: Molecular Characterization of  
741 Water-Soluble Humic like Substances in Smoke Particles Emitted from Combustion of Biomass  
742 Materials and Coal Using Ultrahigh-Resolution Electrospray Ionization Fourier Transform Ion  
743 Cyclotron Resonance Mass Spectrometry, *Environ. Sci. Technol.*, 52, 2575-2585,

- 744 <https://doi.org/10.1021/acs.est.7b06126>, 2018.
- 745 Song, J., Li, M., Fan, X., Zou, C., Zhu, M., Jiang, B., Yu, Z., Jia, W., Liao, Y., and Peng, P. a.:  
746 Molecular Characterization of Water- and Methanol-Soluble Organic Compounds Emitted from  
747 Residential Coal Combustion Using Ultrahigh-Resolution Electrospray Ionization Fourier  
748 Transform Ion Cyclotron Resonance Mass Spectrometry, *Environ. Sci. Technol.*, 53, 13607-13617,  
749 <https://doi.org/10.1021/acs.est.9b04331>, 2019.
- 750 Sun, J. Z., Zhi, G. R., Hitzenberger, R., Chen, Y. J., Tian, C. G., Zhang, Y. Y., Feng, Y. L.,  
751 Cheng, M. M., Zhang, Y. Z., Cai, J., Chen, F., Qiu, Y., Jiang, Z., Li, J., Zhang, G., and Mo, Y.:  
752 Emission factors and light absorption properties of brown carbon from household coal combustion  
753 in China, *Atmos. Chem. Phys.*, 17, 4769-4780, <https://doi.org/10.5194/acp-17-4769-2017>, 2017.
- 754 Tang, J., Li, J., Su, T., Han, Y., Mo, Y., Jiang, H., Cui, M., Jiang, B., Chen, Y., Tang, J., Song,  
755 J., Peng, P. a., and Zhang, G.: Molecular compositions and optical properties of dissolved brown  
756 carbon in biomass burning, coal combustion, and vehicle emission aerosols illuminated by  
757 excitation-emission matrix spectroscopy and Fourier transform ion cyclotron resonance mass  
758 spectrometry analysis, *Atmos. Chem. Phys.*, 20, 2513-2532, [https://doi.org/10.5194/acp-20-2513-](https://doi.org/10.5194/acp-20-2513-2020)  
759 2020, 2020.
- 760 Wang, Q. Q., Zhou, Y. Y., Ma, N., Zhu, Y., Zhao, X. C., Zhu, S. W., Tao, J. C., Hong, J., Wu,  
761 W. J., Cheng, Y. F., and Su, H.: Review of Brown Carbon Aerosols in China: Pollution Level, Optical  
762 Properties, and Emissions, *J. Geophys. Res.: Atmos.*, 127, <https://doi.org/10.1029/2021JD035473>,  
763 2022.
- 764 Wei, W., Xie, Q., Yan, Q., Hu, W., Chen, S., Su, S., Zhang, D., Wu, L., Huang, S., Zhong, S.,  
765 Deng, J., Yang, T., Li, J., Pan, X., Wang, Z., Sun, Y., Kong, S., and Fu, P.: Dwindling aromatic  
766 compounds in fine aerosols from chunk coal to honeycomb briquette combustion, *Sci. Total*  
767 *Environ.*, 838, <https://doi.org/10.1016/j.scitotenv.2022.155971>, 2022.
- 768 Wozniak, A. S., Bauer, J. E., Sleighter, R. L., Dickhut, R. M., and Hatcher, P. G.: Technical  
769 Note: Molecular characterization of aerosol-derived water soluble organic carbon using ultrahigh  
770 resolution electrospray ionization Fourier transform ion cyclotron resonance mass spectrometry,  
771 *Atmos. Chem. Phys.*, 8, 5099-5111, <https://doi.org/10.5194/acp-8-5099-2008>, 2008.
- 772 Xie, M. J., Hays, M. D., and Holder, A. L.: Light-absorbing organic carbon from prescribed  
773 and laboratory biomass burning and gasoline vehicle emissions, *Sci. Rep.*, 7,  
774 <https://doi.org/10.1038/s41598-017-06981-8>, 2017.
- 775 Xiong, R., Li, J., Zhang, Y., Zhang, L., Jiang, K., Zheng, H., Kong, S., Shen, H., Cheng, H.,  
776 Shen, G., and Tao, S.: Global brown carbon emissions from combustion sources, *Environ. Sci.*  
777 *Ecotechnology*, 12, 100201, <https://doi.org/10.1016/j.ese.2022.100201>, 2022.
- 778 Yokelson, R. J., Susott, R., Ward, D. E., Reardon, J., and Griffith, D. W. T.: Emissions from  
779 smoldering combustion of biomass measured by open-path Fourier transform infrared spectroscopy,  
780 *J. Geophys. Res.: Atmos.*, 102, 18865-18877, [10.1029/97jd00852](https://doi.org/10.1029/97jd00852), 1997.
- 781 Yue, S., Zhu, J., Chen, S., Xie, Q., Li, W., Li, L., Ren, H., Su, S., Li, P., Ma, H., Fan, Y., Cheng,  
782 B., Wu, L., Deng, J., Hu, W., Ren, L., Wei, L., Zhao, W., Tian, Y., Pan, X., Sun, Y., Wang, Z., Wu,  
783 F., Liu, C.-Q., Su, H., Penner, J. E., Poschl, U., Andreae, M. O., Cheng, Y., and Fu, P.: Brown carbon  
784 from biomass burning imposes strong circum-Arctic warming, *One Earth*, 5, 293-304,  
785 <https://doi.org/10.1016/j.oneear.2022.02.006>, 2022.
- 786 Zhang, L., Luo, Z., Du, W., Li, G., Shen, G., Cheng, H., and Tao, S.: Light absorption properties  
787 and absorption emission factors for indoor biomass burning, *Environ. Pollut.*, 267,  
788 <https://doi.org/10.1016/j.envpol.2020.115652>, 2020.
- 789 Zhang, L., Luo, Z. H., Li, Y. J., Chen, Y. C., Du, W., Li, G., Cheng, H. F., Shen, G. F., and Tao,  
790 S.: Optically Measured Black and Particulate Brown Carbon Emission Factors from Real-World  
791 Residential Combustion Predominantly Affected by Fuel Differences, *Environ. Sci. Technol.*, 55,

---

792 169-178, <https://doi.org/10.1021/acs.est.0c04784>, 2021a.

793 Zhang, L., Luo, Z., Xiong, R., Liu, X., Li, Y., Du, W., Chen, Y., Pan, B., Cheng, H., Shen, G.,  
794 and Tao, S.: Mass Absorption Efficiency of Black Carbon from Residential Solid Fuel Combustion  
795 and Its Association with Carbonaceous Fractions, *Environ. Sci. Technol.*, 55, 10662-10671,  
796 <https://doi.org/10.1021/acs.est.1c02689>, 2021b.

797 Zhang, L., Hu, B., Liu, X., Luo, Z., Xing, R., Li, Y., Xiong, R., Li, G., Cheng, H., Lu, Q., Shen,  
798 G., and Tao, S.: Variabilities in Primary N-Containing Aromatic Compound Emissions from  
799 Residential Solid Fuel Combustion and Implications for Source Tracers, *Environ. Sci. Technol.*,  
800 <https://doi.org/10.1021/acs.est.2c03000>, 2022.

801 Zhao, Y., Hallar, A. G., and Mazzoleni, L. R.: Atmospheric organic matter in clouds: exact  
802 masses and molecular formula identification using ultrahigh-resolution FT-ICR mass spectrometry,  
803 *Atmos. Chem. Phys.*, 13, 12343-12362, <https://doi.org/10.5194/acp-13-12343-2013>, 2013.

804

805